Journal of Applied Mechanics Vol. 5, pp. 591-600 (August 2002) JSCE

Numerical simulation on crust deformation due to CO_2 sequestration in deep aquifers

CO_2地中貯留における地盤の力学安定性に関する数値解析的検討

Qi Li[1], Zhishen Wu[2], Xiaochun Li[3], Takashi Ohsumi[4] and Hitoshi Koide[5]
李 琦・呉 智深・李 小春・大隅 多加志・小出 仁

[1] Dr. Candidate of Eng., Dept. of Urban & Civil Eng., Ibaraki University
(4-12-1, Nakanarusawa-cho, Hitachi, Ibaraki 316-8511)
[2] Dr. of Eng., Professor, Dept. of Urban & Civil Eng., Ibaraki University
(4-12-1, Nakanarusawa-cho, Hitachi, Ibaraki 316-8511)
[3,4,5]Dr. of Eng., Research Institute of Innovative Technology for the Earth
(9-2 Kizugawadai, Kizu-cho, Soraku-gun, Kyoto 619-0292)

In Japan, deep brine aquifers in sedimentary basins have a huge sequestration capacity and extensive distribution, therefore, sequestration of carbon dioxide (CO_2) in deep aquifers is one of the variable and feasible options for CO_2 emission cutting. (Tanaka et al., 1995; Koide, 1999). However, the injection of CO_2 may considerably modify the stress state in the subsurface and result in the deformation and even failure along the previously existing soft bands, especially the fault, in the strata. Although most researches have been carried out about the process of CO_2 injection, the interaction between CO_2 and water, and the seepage of CO_2 in the formations, the research is rarely touched on the reaction of the fault around the storage site after the CO_2 injection. Our research in this area is focused on the stress variation and deformation around the storage strata after the CO_2 injection, especially its effects on the fault. An FEM simulator was constructed with considerations of the initial stress, pore pressure, and fault. This paper reports our recent efforts in developing such a simulator and some preliminary simulation results. These preliminary simulations have been conducted to investigate the CO_2-driven buoyancy stress distribution, injection force and the influence process of CO_2 injection on the fault under different positions and different dip angles. At last some interesting results are concluded.

Key Words: Carbon dioxide, Sequestration, Deep aquifer, Fault, Numerical simulation

1. Introduction

Our planet is warming by the greenhouse effect mainly caused by carbon dioxide (CO_2), which is responsible for about 64% (Bryant, 1997), in the atmosphere year by year. As a result of mankind activities, the concentration of CO_2 in the atmosphere had risen from a relatively stable level around 275 ppmv in the pre-industrial era to about 355 ppmv in 1994 (Houghton, 1994). Currently it continues to rise at rates of about 1.8 ppmv per year. Thus, the world has a strong interest in reducing CO_2 emissions into the atmosphere while at the same time ensuring sustainable economic development. A general mitigation of carbon dioxide emissions involves basically three approaches: (1) improved or alternate energy use; (2) the capture and utilization of CO_2; or (3) the long-term disposal of carbon dioxide. (Bachu, 1996; 2000) The third approach is widely adopted as a safe, technically feasible, cost-effective and socially acceptable method of the reduction of CO_2. Then long-term and safe sequestration of CO_2 is fast becoming an urgent demand. A number of disposal methods are currently being studied. These can be divided into three main categories, ocean, terrestrial and geologic disposal, with retention times of the order of $10\text{-}10^5$ years, respectively (Gunter et al., 1998). Underground disposal in aquifers is regarded as a promising method of disposing of very large quantities of CO_2. The existing estimates show 73.5 billion tons of CO_2 potential capacity in offshore aquifers near Japan Islands Arc. (Tanaka et al., 1995; Kaya and Koide et al., 1999)

The primary processes affecting the injection and

geological sequestration of CO_2 can be concluded as: (1) multiphase, radial injection of CO_2 and the growth of the CO_2 bubble around the injector with time, (2) buoyancy-driven migration of CO_2 toward the overlay confining aquifer, (3) escape of CO_2 through leakage, (4) dissolution of CO_2 during injection and vertical migration, and the resulting aqueous speciation of carbon, (5) carbon mass exchange via precipitation and dissolution of minerals through the interaction of dissolved and gaseous phase CO_2 with the formation, (6) changes in hydrogeological properties due to mineral trapping and the resulting formation damage, injectivity decline and fracturing. So far many researches have been carried out to investigate the flow and transport process of carbon dioxide, the interaction between CO_2 and water and the seepage of CO_2 in the formations. Weir et al. (1995) proposed a numerical modeling study of CO_2 injection and sequestration using the code TOUGH2, without considering the escape of CO_2 through leakage and its dissolution. Law and Bachu (1996) performed a hydrogeological and a two-dimensional numerical analysis of CO_2 disposal in deep aquifers in the Alberta sedimentary basin to assess the hydrodynamic trapping capacity of two aquifers in Canada. McPherson and Cole (2000) also used the TOUGH2 simulator to model the sequestration of CO_2 in the Powder River Basin of Wyoming, USA. McPherson and Lichtner (2001) used a mathematical sedimentary basin model, including multiphase flow of CO_2, groundwater, and brine, to evaluate residence times in possible aquifer storage sites and migration patterns and rates. They also simulated CO_2 flow through fractures, to evaluate partitioning between fractures and rock matrix. Saripalli et al. (2001) used a numerical model (STOMP-CO_2) for the simulation of deep well injection of CO_2 and simulated the CO_2 bubble growth with time. Ferer et al. (2001) constructed a pore-level model of carbon dioxide sequestration in brine fields and it has been used with experimental values of interfacial tensions and a range of possible viscosities, to study the injection of CO_2 into brine-saturated porous media, at high pressures. Sminchak et al. (2001) evaluated the issues related to seismic activity induced by the injection of CO_2 in deep saline aquifers in USA.

In the past few years a considerable research programs have been pushed ahead in USA, Europe and Australia. In 2000, Japan formally launched a 5-year national R&D program of "Underground Storage of Carbon Dioxide" under the auspices of New Energy and Industrial Technology Development Organization. A small-scale field test of liquid CO_2 injection at an onshore gas/oil field site will be conducted until 2004 in Japan. As we know, Japan Islands Arc is located in a tectonically active region, with complex geologic conditions and dense faults. Thus the mechanical stability is of great importance for safety evaluation of the geological sequestration of carbon dioxide, especially the consideration of faults around the CO_2 storage site. The effects of these faults must be evaluated with respect to the potential for induced seismicity and leakage associated with seismic events.

Although a lot of researches have been made as reviewed above, the effect on the top rock and the fault around the storage site after the CO_2 injection has not yet been thoroughly studied until now. In this paper, we mainly focus on clarifying the influence of CO_2 on deformation behavior and possible failure-slip mechanism of the overlying strata and the fault. Here a general-purpose FEM code of ABAQUS is applied to simulate the behavior of the overlying strata with or without a fault after the CO_2 bubble is relatively stable in the aquifer (feasible if considering a relatively short geological time). In ABAQUS, modeling of possible-slip on the fault is treated as a contact problem, and the fault is defined by the flexible joint spring method.

2. Geological Model

In our research, a typical model of geological media for CO_2 disposal in a deep aquifer is considered. Fig. 1 shows the two-dimensional cross section of the test model of the CO_2 disposal system.

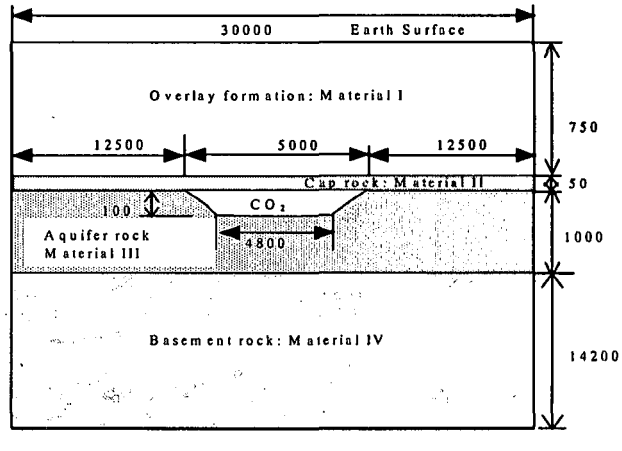

Fig.1 Geological model without fault (unit: m)

The size of the model is 30000m laterally and 16000m vertically in order to eliminate the boundary effect on the simulation results. The storage aquifer is at the

depth of 800m and the injected CO_2 bubble is 5000m wide along the bottom of cap rock and 100m thick. In the latter analysis the thickness of CO_2 will be enlarged. Table 1 shows the properties of all materials used in the FEM analysis.

Table 1 Properties of geological materials

Material	Parameters	Value (SI Unit)
Overlay Formation (Material I)	Young's Modulus	2.0E+9
	Poisson's ratio	0.25
	Density	2100
Cap Rock (Material II)	Young's Modulus	4.0E+9
	Poisson's ratio	0.25
	Density	2100
Aquifer Rock (Material III)	Young's Modulus	4.0E+10
	Poisson's ratio	0.25
	Density	2100
Basement Rock (Material IV)	Young's Modulus	1.0E+11
	Poisson's ratio	0.25
	Density	2600
Water	Density	1000
CO_2	Density	600

In this paper the model with a fault is given emphasis to investigate its potential effect on the mechanical behavior of the strata. Four typical fault cases, which have a dip angle of 45 degree and which extend to the cap rock, are studied according to the distance from the deep end of the fault to the left forefront of the CO_2 bubble. Fig. 2 and Table 2 show the four cases.

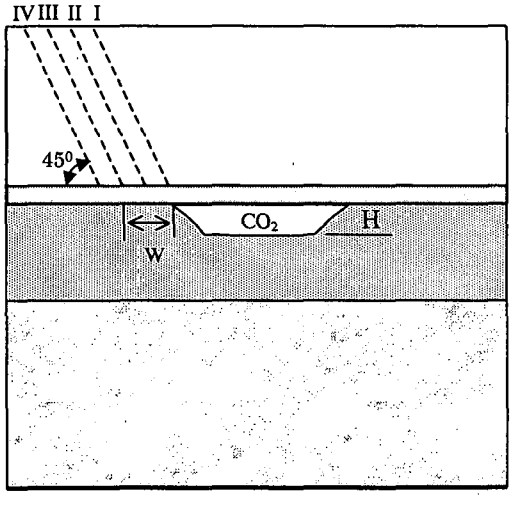

Fig.2 Sketch of four fault cases

Table 2 Four cases of the fault position

Case	Value of W (m)
I	0
II	500
III	2500
IV	7500

The fault for all of four cases has the same normal stiffness and shear stiffness, shown in Table 3. The properties of the fault are quite site specific. The values of normal and shear stiffness are chosen mainly following a report about the fault property of Kinki area of Japan [25].

Table 3 Properties of the fault

Parameters	Value (SI Unit)
Normal stiffness	2.0E+7
Shearing stiffness	1.0E+7

As we know, the geological materials are under the effect of gravity during the geological long time. If the gravity acts upon the subsurface material, which has the Poisson's ratio not equal to 0.5, the differential stress is generated. Thus it is important to consider the initial stress in the coming analysis. Fig. 3 shows the horizontal and vertical stress distribution applied in the initial stress iteration process.

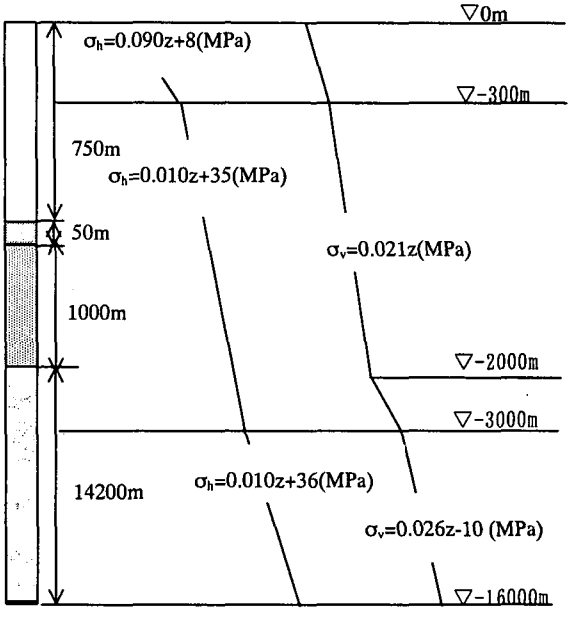

Fig.3 Initial stress distribution applied in formations

3. Numerical Simulations

A model is constructed representing a typical brine reservoir that might be considered as a candidate for the CO_2 sequestration in our FEM analysis. A normal fault is placed into the model and following the position discussed above. Fig. 4 shows a finite element mesh of the structural model. The model is consisted of 4-noded isoparametric, quadratic elements and assumed a condition of plane strain. The two surfaces of the fault are linked by 13 flexible spring elements. A zero displacement boundary condition, Ux=0, is used along the vertical sides, Ux=Uy=0 along

the base of the model. The upper surface of the model is free.

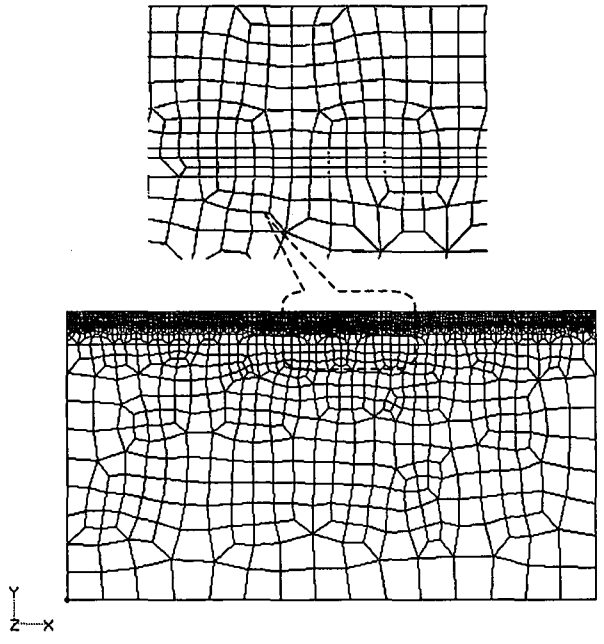

Fig.4 Mesh of FEM model

3.1 CO_2 Bubble Driven Buoyancy

Due to the density difference between water and CO_2, the supercritical CO_2 bubble will eventually float toward the cap rock layer. The density driven flow finally results in the birth of buoyancy at the bottom of the confining cap rock layer. In our research the change of the pore pressure in the aquifers is reflected by the buoyancy in the CO_2-occupied zone. The pore pressure at any point in this zone is $P_{CO2}=gz\rho_w+g(\rho_w-\rho_{CO2})\xi$, shown in Fig. 5, where g is the gravity acceleration, ρ_w is the density of water, ρ_{CO2} is the density of supercritical CO_2, z is the depth of the point from the earth surface and ξ is the vertical distance from the lower edge of the CO_2-occupied zone to that point.

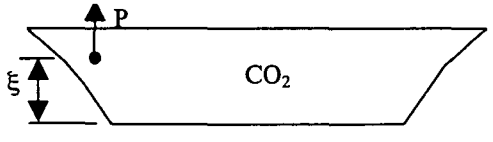

Fig.5 Pore pressure change in the CO_2-occupied zone

3.2 Impact of Injection

Here, in order to consider the effect of the injection force on the strata, the response to an increase of the pore pressure within the whole storage aquifer (material III) is illustrated as shown in Fig. 6.

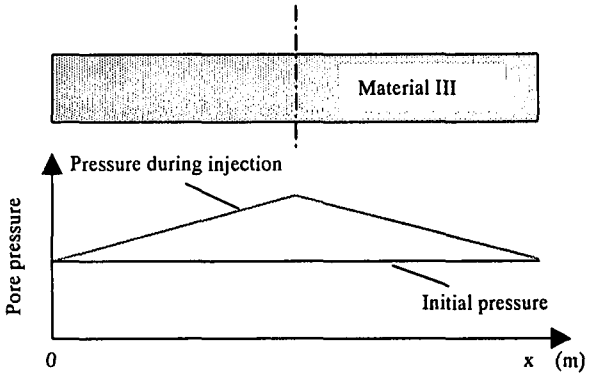

Fig.6 The pore pressure distribution in the storage aquifer prior to and during the injection.

During the injection, the pore pressure distribution (P) in the whole aquifer varies according the following equations:

$P= 0.01z\,(1 + 0.2x/15000)$
$(800 \le z \le 900m,\ 0 \le x \le 15000m)$
$P= 0.01z\,(1.4 - 0.2x/15000)$
$(800 \le z \le 900m,\ 15000 \le x \le 30000m)$

3.3 Flexible Joint Spring Element on Fault Surface

In ABAQUS, modeling of the status development on the fault can be treated as a contact problem, and the fault is defined by the flexible joint spring method in our research, see Fig. 7.

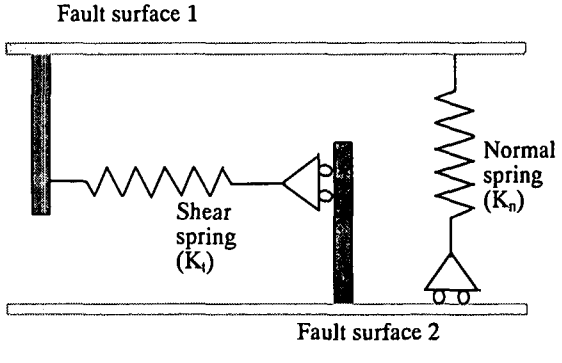

Fig.7 Flexible joint spring model

On the fault surface, the elastic characters of normal component and tangent component can be described by giving the following stiffness matrix as follows.

$$[K]=\begin{bmatrix} -K_t & 0 \\ 0 & -K_n \end{bmatrix}$$

As for elastic behavior along the fault surface, the relationship between the force increment and the relative elastic displacement $\{\Delta(\Delta u)\}$ can be expressed as

$$\{\Delta f\} = [K]\{\Delta(\Delta u)\}$$

3.4 Steps of Simulation

1) In order to avoid the localized large deformation, the initial stress distribution shown above (see Fig. 3) is applied to each element so that the deformation of each element becomes small after the application of gravity.
2) To apply the CO_2 bubble driven buoyancy to elements of the CO_2 occupied zone as distributed force loads.
3) The injection force driven stress change is applied along the bottom of top rock layer as centralized force loads according to the distribution function discussed above (see Section 3.2).
4) To simulate the fluctuation of stress and deformation of the structure model after the force loads are applied.

3.5 Numerical Results and Discussion

(1) Variation of Earth Surface

In order to investigate the effect on the overlying formations above the CO_2 bubble, the different thickness (H, see Fig.2) of the CO_2 bubble is considered from 100m to 250m. The vertical deformation and the gradient change along the top surface of the model are shown in Fig. 8 and Fig. 9. In Fig. 8-a, the maximum deformation of 30 millimeter is achieved. Fig. 8-b is the gradient change according to the Fig. 8-a. Although obviously the change of the surface gradient is so small it should be paid attention to the variation of earth surface. As shown in the following Fig. 9, the vertical deformation change is fast with the incrassation of the CO_2 bubble towards the depth direction, but the gradient change still keeps a small level.

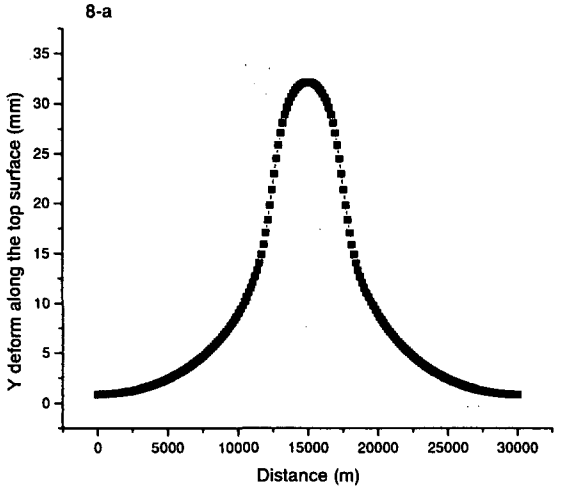

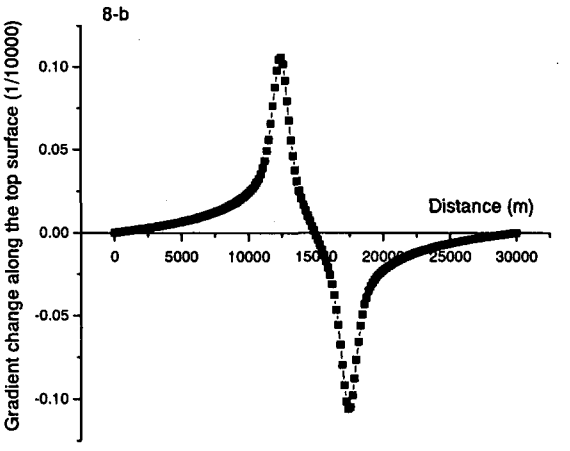

Fig.8 The vertical deformation and surface gradient of the model without a fault under the CO_2 bubble with H=100m

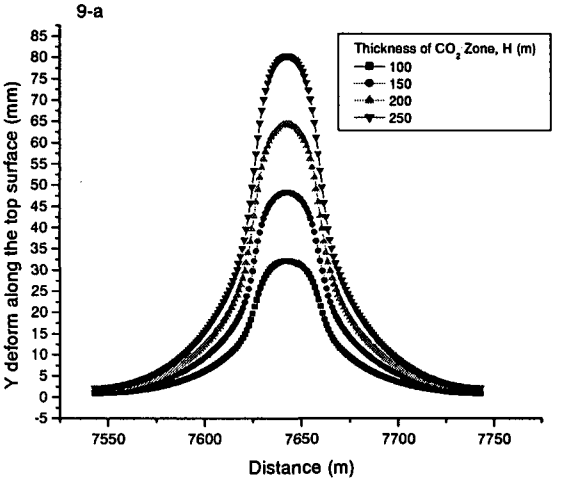

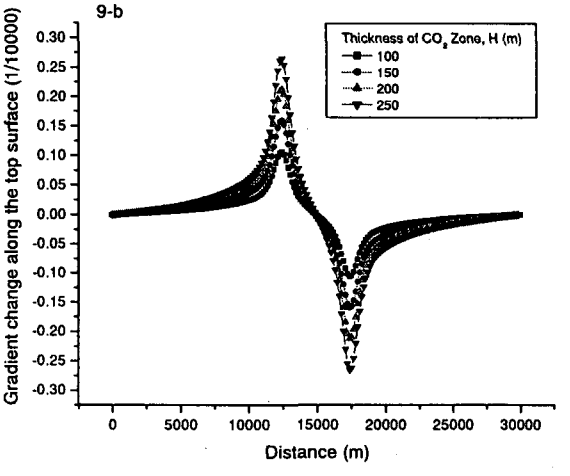

Fig.9 The vertical deformation and the gradient change along the top surface under different sizes of the CO_2 bubble

As mentioned by many researchers, the injection force will evidently change the pore pressure distribution in the aquifer. So the effect on the overlying formations under the injection driven pore pressure and the CO_2 bubble driven buoyancy are compared. From Fig. 10 the difference of the vertical deformation along the top surface is obvious. The injection driven pore pressure has greater influence on the strata deformation than the CO_2 bubble driven buoyancy.

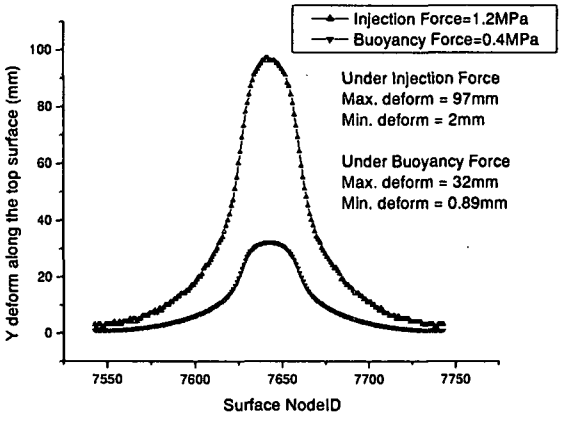

Fig.10 The comparison between injection driven pore pressure and CO_2 bubble driven buoyancy

(2) Influence on Fault due to the CO_2 Injection

As mentioned above, the purpose of our preliminary simulation studies is to investigate the impact on the fault from the CO_2 bubble during a relatively short geological time after the injection, so as to determine the feasibility of injecting a given amount of CO_2 into the geological media. Thus, simulations were focused on considering four different positions of the fault, Case I to Case IV (see Table 2), in accordance with the distance from the CO_2-occupied zone (see Fig. 2). The following Fig. 11-Fig. 14 show the shear stress change and relative slip of nodes on the fault surface under the different size of the CO_2 bubble (H changed from 100m to 250m, see Fig.2), i.e. the different CO_2 bubble driven buoyancy. For Fault Case I, see Fig. 11, with the enlargement of the thickness (H) of the CO_2 bubble, the shear stress on the fault surface increases accordingly. The shear stress is positive, denoting a upward movement of the hanging wall with respect to the footwall. The magnitude of the shear stress is 0.02~0.24 MPa. It is interesting that the maximum value of the shear stress on the fault surface is located at nearly the center of the fault line. The bottom end of fault I is exactly situated on the top of the left forefront of the CO_2 bubble, and only the cap rock is between them. Under such conditions the appearance of the maximum of the shear stress on the fault surface is delayed. The CO_2 bubble driven buoyancy strongly influences the behavior of the fault surface and lead to the cap distribution of the shear stress. The relative slip of nodes on the fault surface is under small millimeter magnitude (Fig.11-b).

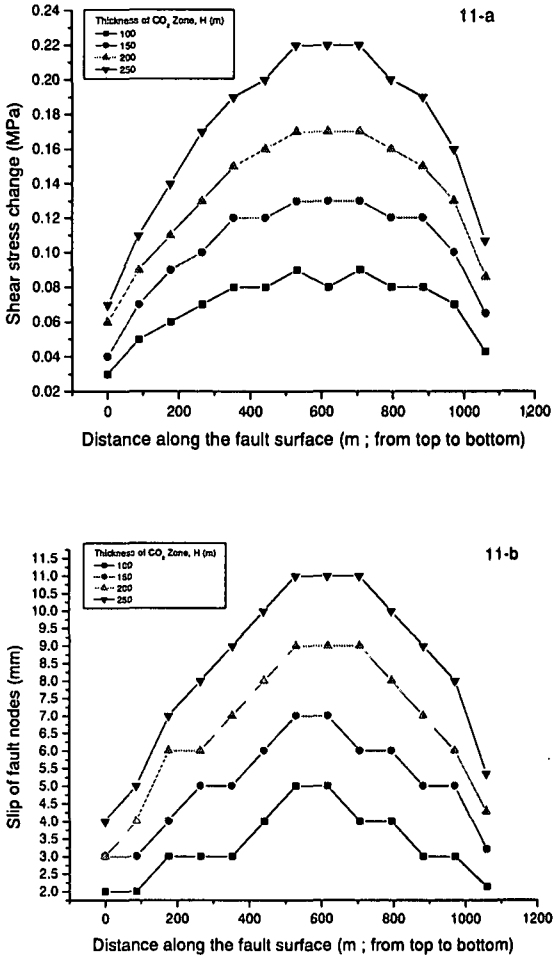

Fig.11 The shear stress change and the relative slip of Fault Case I under buoyancy.

From Fig. 12-a, Fig 13-a and Fig. 14-a, it can be concluded that the shear stress on the fault surface fast decreases and is changed to negative, denoting a downward movement of the hanging wall with respect to the footwall, with far away from the CO_2 bubble.

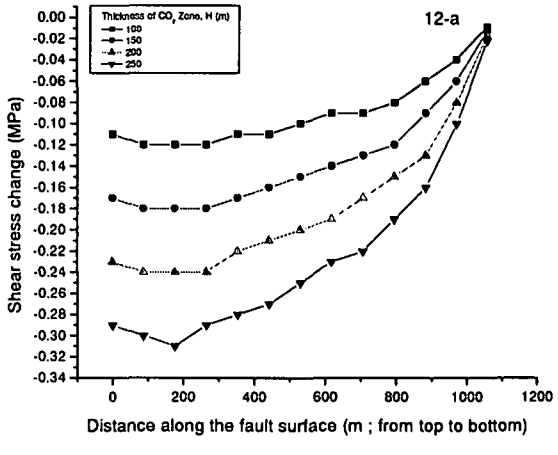

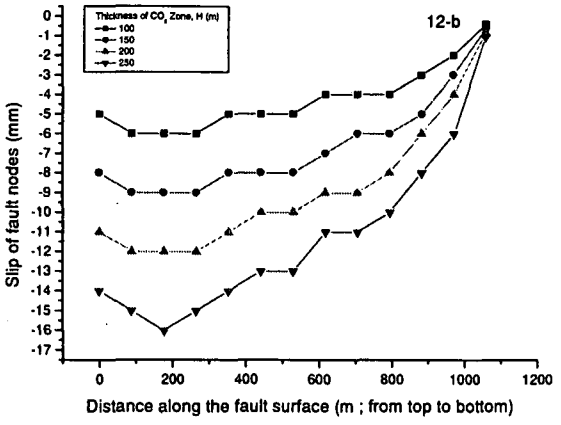

Fig.12 The shear stress change and the relative slip of Fault Case II under buoyancy.

It seems that the trend of the shear stress on the fault surface quickly becomes stable, and exhibits the comet distribution. This can be obvious represented by Fig. 12-a, Fig.13-a and Fig.14-a. The relative slip of nodes on the fault surface also exhibits the millimeter magnitude (Fig.12-b, Fig.13-b, Fig.14-b).

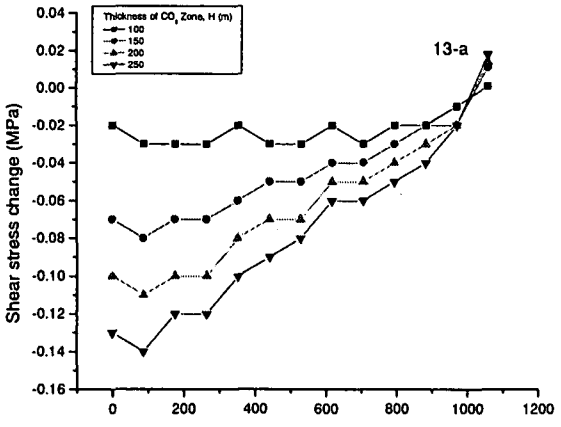

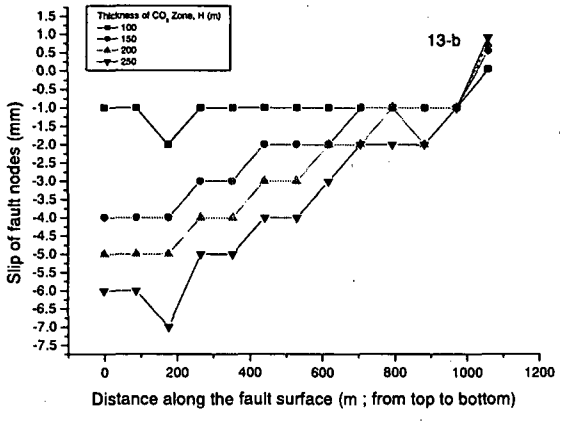

Fig.13 The shear stress change and the relative slip of Fault Case III under buoyancy.

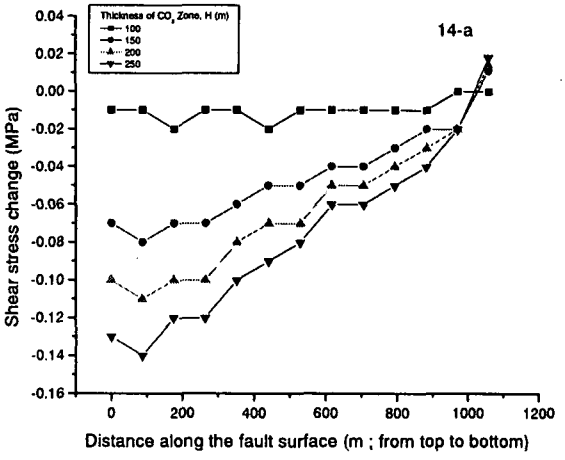

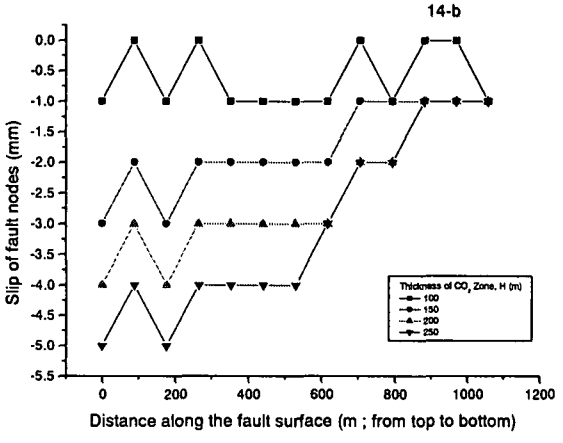

Fig.14 The shear stress change and the relative slip of Fault Case IV under buoyancy.

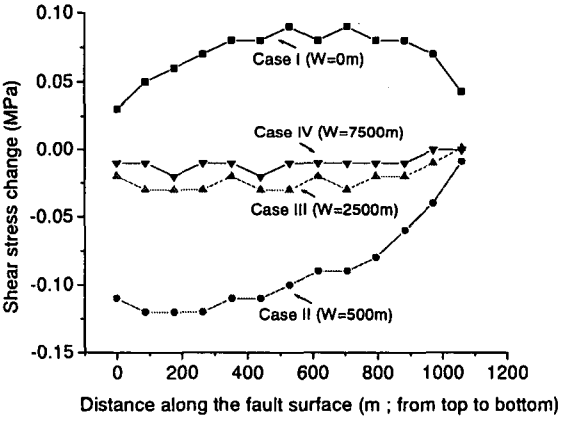

Fig.15 Shear stress change of four fault cases under the CO_2 bubble with H=100m

From the discussion above, the fault is located in the area very near the CO_2 bubble should been given enough attention for the purpose of safety. Fig. 15 demonstrates again the influence from

the CO_2 bubble on the fault. The influence fast declines when the fault is becoming far away from the CO_2 bubble.

On the other hand, under the CO_2 bubble with H=100m, the response of the fault, Case I, with different values of the tangent stiffness, Kt, was performed. The result is shown in Fig. 16. With increase of the value Kt, the shear stress on the fault surface is declined accordingly. But the influence of the property Kt of the fault, i.e. the tangent stiffness, is not evident comparing with the size of the CO_2 bubble. This factor should be given a consideration when evaluating a storage site for the CO_2 geological disposal.

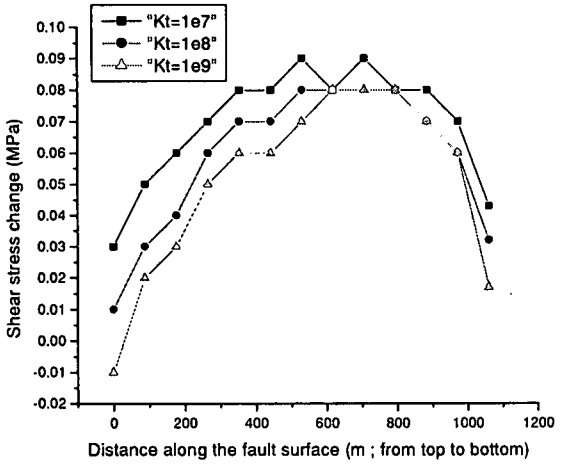

Fig.16. Shear stress decline on the fault with the increase of tangent stiffness, Kt

In order to study the effect of the CO_2 bubble on the different dip fault, the dip angle of fault case I varied with four situations, namely, 15^0, 30^0, $45^0$and 60^0, was investigated.

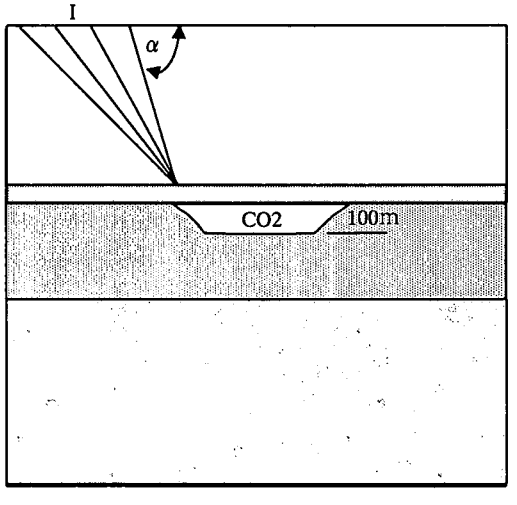

Fig.17 Sketch map of fault case I under different dip angles

The sketch map is shown in Fig.17, and Fig.18 shows the shear stress change and relative slip of the bottom end node of the fault. Only from Fig.18 it can be concluded that the dangerous fault is the one with the dip angle 45^0 under the same CO_2 bubble.

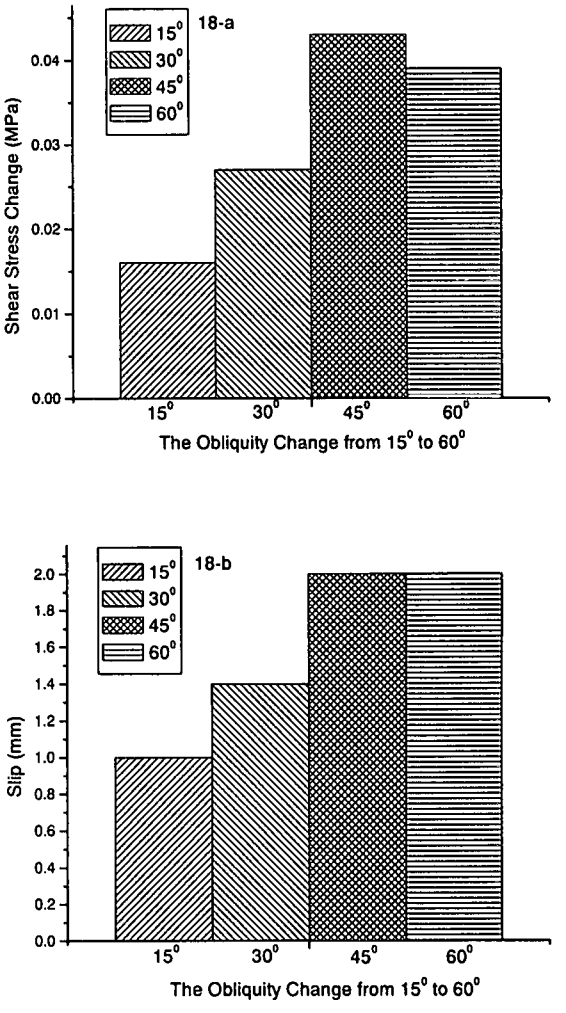

Fig.18 Shear stress change and relative slip of the bottom end node of the fault under different dip angles.

4. Conclusions and Future Work

In this paper we used ABAQUS-based finite element models with elastic material properties both in the continuous body and on the fault surface to simulate the influence of the CO_2 bubble driven buoyancy on the overlying formations, especially on the fault surface, after the injection of CO_2 into the deep aquifers for a relatively short geological time. From our research discussed above, it appears at this current stage that there are no obvious geological reasons that would make CO_2 sequestration in the deep aquifers unworkable if the process of the site choosing is thoroughly considered and the FEM analysis is also better pre-performed. The following is some preliminary suggesting conclusions:

(1) The CO_2 bubble driven buoyancy has no evident influence on the gradient change along the top earth surface and the fault stability with the thickness of the bubble enlarging from

100m to 250m. But the vertical deformation along the top earth surface should be paid attention to.

(2) Relative to the CO_2 bubble driven buoyancy the injection force driven pore pressure change has much more influence on the overlying formations.

(3) The shear stress on the fault surface fast decreases with far away from the CO_2 bubble. And the trend of the shear stress on the fault surface quickly becomes stable, and exhibits the comet distribution.

(4) Comparing with the shear stiffness of the fault the CO_2 bubble size itself should be given much more considerations when evaluating a storage site for the CO_2 geological disposal.

(5) The fault located in the area very near the CO_2 bubble should be given enough attention for the purpose of safety.

(6) The shear stress change and relative slip on the fault surface is influenced by the dip angle of the fault.

It is important to restate that most of the process of the CO_2 injection into the geological media are site specific, so the finite element method, which involves several assumptions concerning the fault strength and the CO_2 bubble, provides less certainty than direct evidence from monitoring instruments.

In the future the assessment of the fractured rock formations under the injection of CO_2 should be involved. Meanwhile the in-situ monitoring should be performed so as to rectify the parameters in our FEM analysis. Ultimately the induced seismic activity along the previously fractured zone, for example the fault, with the disposal of CO_2 into deep brine aquifers should be considered.

References

1) ABAQUS/Standard User's Manual 5.8, H. K. S. Inc., USA, 1998

2) Bachu, S., and Hitchon, B., Regional-scale flow of formation waters in the Williston Basin, *American Association of Petroleum Geologists Bulletin*, 80, pp. 248-264, 1996

3) Bachu, S., Sequestration of CO_2 in geological media: criteria and approach for site selection in response to climate change, *Energy Conversion and Management*, 41, pp. 953-970, 2000

4) Bryant, E., *Climate Process and Change*, Cambridge University Press, Cambridge, U. K., 1997

5) Ferer, M., et al., Pore-level modeling of carbon dioxide sequestration in brine fields, *Proc. of First National Conference on Carbon Sequestration*, 2001

6) Gunter, W. D., Wong, S., Cheel, D. B., and Sjostrom, G., 1998, Large CO_2 sinks: their role in the mitigation of greenhouse gases from an international, national (Canadian) and provincial (Alberta) perspective, *Applied Energy*, 61, pp. 209-227, 1998

7) Hendriks, C. A. and Blok, K., Underground storage of carbon dioxide, *Energy Conversion and Management*, 34, pp. 949-957, 1993

8) Hitchon, B., *Aquifer Disposal of Carbon Dioxide*, Geoscience Publishing Ltd., Canada, 1996

9) Houghton, J. T., *Global Warming: The Complete Briefing*, Lion Publishing plc, Oxford, England, 1994

10)Jane., C.S..L, *Rock Fractures and Fluid Flow*, National Academy Press, Washington, D. C., 1996

11)Kaya, Y., Koide, H., and et al., Underground sequestration of carbon dioxide in tectonically active area, *Greenhouse Gas Control Technologies*, pp. 296-298,1999

12)Koide, H., Geotechnical challenges to geological hazard and protection of environment, keynote paper, *Proc. Of the 8th International Congress on Rock Mechanics*, A.A. Balkema, Rotterdam, pp.1005-1012, 1997

13)Koide, H., Geological Sequestration and Microbiological Recycling of CO_2 in Aquifers, *Greenhouse Gas Control Technologies*, pp. 201-205,1999

14)Koide, H., et al., Deep Sub-seabed Disposal of CO_2 – The Most Protective Storage, *Energy Conversion and Management*, 38, pp. 253-258, 1997

15)Koide, H., Tazaki, Y., Noguchi, Y., Iijima., M., Ito., K;., and Shindo, Y., Underground storage of carbon doxide in depleted natural gas reservoirs and in useless aquifers. *Engineering Geology*, 34, pp. 175-179, 1993

16)Law, D. H. –S. and Bachu, S., Hydrogeological and numerical analysis of CO_2 disposal in deep aquifers in the Alberta sedimentary basin, *Energy Conversion and Management*, 37, pp. 1167-1174, 1996

17)McPherson, B.J.O.L and Cole, B. S., Multiphase CO_2 flow, transport and sequestration in the Powder River basin, Wyoming, USA, *Journal of Geochemical Exploration*, 67-70, pp.65-69, 2000

18)McPherson, B.J.O.L and Lichtner, P. C., CO_2 sequestration in deep aquifers, *Proc. of First National Conference on Carbon Sequestration*, 2001

19)Rybal'chenko, A.I., et al., *Deep Injection Disposal of Liquid Radioactive Waste in Russia*, Battele Press, Columbus, Ohio, USA, 1998.

20)Saripalli, K. P., McGrail, B. P., and White, M. D, Modeling the sequestration of CO_2 in deep geological formations, *Proc. of First National Conference on Carbon Sequestration*, 2001

21)Sminchak, J. R., Gupta, N., Byrer, C., and Bergman, P., Issues related to seismic activity induced by the injection of co_2 in deep saline aquifers, *Proc. of First National Conference on Carbon Sequestration*, 2001

22)Sugawara, K., Measuring rock stress and rock engineering in Japan, *Rock Stress*, pp. 15-24, Balkema, Rotterdam, 1997.

23)Tanaka, S., Koide, H., and Sasagawa, A., Possibility of

underground CO_2 sequestration in Japan, *Energy Conversion and Management*, 36, pp. 527-530, 1995
24)Weir, G.J., White, S. P., and Kissling, W. M., Reservoir storage and containment of greenhouse gases, *Energy Conversion and Management*, 36, pp. 531-534, 1995
25)平成 11 年度, 「低レベル放射性廃棄物処分可視画像化調査報告書 （平成 3～11 年度検討の総括）」, 財団法人 原子力環境整備センター, 平成 12 年 3 月.

(Received April 19, 2002)